Journal of Molecular Structure 976 (2010) 371–376

Contents lists available at ScienceDirect

Journal of Molecular Structure

journal homepage: www.elsevier.com/locate/molstruc

C=N—N=C conformational isomers of 2′-hydroxyacetophenone azine: FTIR matrix isolation and DFT study

Joanna Grzegorzek, Zofia Mielke *, Aleksander Filarowski

Faculty of Chemistry, University of Wrocław, Joliot Curie 14, 50-383 Wrocław, Poland

ARTICLE INFO

Article history:
Received 9 February 2010
Received in revised form 9 March 2010
Accepted 13 April 2010
Available online 20 April 2010

Keywords:
Azine
Infrared spectra
Matrix isolation
Conformational analysis
Theoretical calculation
Hydrogen bonding

ABSTRACT

2′-hydroxyacetophenone azine (APA) has been studied by matrix isolation infrared spectroscopy and quantum chemical calculations. The DFT/B3LYP/6-311++G(2d,2p) calculations demonstrated the existence of two conformers for the lowest energy *E*/*E* configuration of APA, a *s-trans* and a *gauche* ones. The conformers are characterized by similar energies and differ in the value of a C=N—N=C angle, that was calculated to be 180° for a planar *s-trans* conformer and 155° for a non-planar *gauche* one. The calculated barrier for conformational interconversion is also very low, ca. 1 kJ mol^{-1} for the conversion from a *gauche* conformer to a *trans* one. The FTIR spectra of an argon matrix doped with APA from a vapour above solid sample evidence the presence of both conformers that exhibit reversible interconversion at matrix temperatures. The comparison of the theoretical spectra with the experimental ones and reversible temperature dependence of the experimental spectra allowed for unambiguous spectroscopic characterization of the *trans* and *gauche* conformers. The experiment also demonstrated that a *gauche* conformer is more stable than a *trans* one. The spectra analysis indicates that transformation from a *trans* conformer to a *gauche* one weakens the intramolecular O—H···N bonds in the molecule.

1. Introduction

Azines, and in particular aromatic azines, are receiving increasing attention for their biological, chemical and physical properties [1–4]. They play an important role in synthetic chemistry [5,6] and are potential nonlinear optical materials [7,8]. A series of salicylaldehyde azine derivatives were found to exhibit interesting aggregation-induced emission enhancement characteristics that is a promise of their potential applications in such devices like optical sensors or light emitting diodes [9].

In light of the great utility of aromatic azines, there has been significant interest in studies of their stereochemistry and isomerism [8,10–17]. Most of the experimental studies were performed for the crystalline state [12]; recently a number of quantum chemical calculations that refer to the gaseous state has been also reported [14,15]. A survey of the conformations of a number of derivatives of the parent compound benzaldazine was given recently by van Schalkwyk and Stephen [12].

The conformation of aromatic azine is controlled by the chain of four atoms: C=N—N=C as depicted in Scheme 1.

Almost all studied aromatic azines exist in the preferred (E,E) configuration in which the large groups attached to the C=N bonds are *trans* to the N—N one. The stereochemistry of the azines with respect to the N—N single bond is determined by the τ_1 angle, for a *s-trans* conformation $\tau_1 = 180°$ and for a *gauche* one $\tau_1 \neq 180°$; in the s-*trans* conformation conjugation of two halves of azine is at a maximum. Most of the crystal structures of azines show either N—N s-*trans* or *gauche* conformation, only in a few cases both conformations occur in polymorphous crystals. The most marked conformational changes result from substitution of various bulky groups for H on the azine carbon atoms. The set of compounds containing the group [ArCMe=N—]$_2$ (Ar – differently substituted aromatic rings, Me – methyl group) is markedly different structurally from the set involving the [ArCH=N—]$_2$ group [12]. The steric hindrance of Me group in the first set of compounds causes distortion about the N—N bond which results in τ_1 value strongly deviating from 180° and the general form of the molecule in some cases approximates rather to an orthogonal than to a planar structure. There are, however, exceptions from this general trend. The crystal structure of 2′-hydroxyacetophenone azine (which involves [(o-OHAr)CMe=N—]$_2$ group) consists of discrete almost planar molecules characterized by the τ_1 value equal to 177°. This no doubt follows from the strong O—H···N bonding of the O—H group to N [18].

The 2′-hydroxyacetophenone azine (APA) is a derivative of salicylaldehyde azine (SAA) in which the two hydrogen atoms at azine carbons [(o-OHAr)CH=N—]$_2$ are replaced by methyl groups. The salicylaldehyde azine is the smallest possible symmetric aromatic Schiff base with two hydrogen bonding centres and the

* Corresponding author. Tel.: +48 71 3757475; fax: +48 71 3282348.
E-mail address: zm@wchuwr.chem.uni.wroc.pl (Z. Mielke).

0022-2860/$ - see front matter © 2010 Elsevier B.V. All rights reserved.
doi:10.1016/j.molstruc.2010.04.017

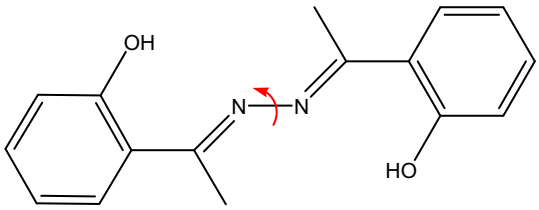

Scheme 1.

molecule was a subject of many studies [19]. In contrast with SAA there are only few literature data on APA properties; the structural characteristics [17,18,20] and the infrared and Raman spectra of the molecule in the crystalline state have been recently reported [16,17,21]. We performed the FTIR matrix isolation study and DFT/B3LYP calculations of APA with the aim to obtain characteristics on its low energy conformers. The calculations performed for the methyl(*para*-methylphenyl) ketone azine [11] demonstrated that the activation energy required for τ variations between the N—N s-*trans* and *gauche* structures is very small, below 0.5 kcal mol^{-1} for this compound. If the potential energy barrier between the two lowest conformers of APA lies also below 1 kJ mol^{-1} the two conformers should be in conformational equilibrium in the matrix [22]. Matrix isolation has been proved to be extremely powerful technique in the conformational study.

2. Experimental section

2.1. Infrared matrix isolation studies

The APA/Ar matrix was obtained by simultaneous deposition of vapour above solid APA, kept at 333 K, and argon on a gold-plated copper mirror kept at 17 K by a closed cycle helium refrigerator (Air Products, Displex 202A). The matrix concentration was controlled by the matrix gas flow rate that was adjusted to minimize the concentration of APA dimers and higher aggregates. The spectra were recorded for the matrix kept at 9 K, 17 K and 32 K; after deposition at 17 K the matrix was cooled down to 9 K, then heated to 32 K and again cooled down to 9 K.

The infrared spectra (resolution 0.5 cm^{-1}) were recorded in a reflection mode with Bruker 113v FTIR spectrometer using a MCT detector cooled by liquid N_2.

The synthesis of 2′-hydroxyacetophenone azine was performed from 2:1 stoichiometric mixtures of 2-hydroxyacetophenone and saturated ammonia water solution in methanol according to Furnuss et al. [23].

2.2. Computational methods

The calculations were performed with the Gaussian03 suite of programs [24]. The DFT/B3LYP/6-311++G(2d,2p) method was applied to optimize all the structures and to calculate the harmonic frequencies. Binding energies were corrected by the Boys-Bernardi full counterpoise correction [25]. Potential-energy torsional profiles were obtained by optimizing all geometrical parameters except for the CNNC torsional angle that was fixed at a given value (using increments of 5°).

All the stationary points were unambiguously characterized as minima or transition states by their vibrational spectra. The computed harmonic frequencies were scaled down by a single factor 0.982 to correct them for the basis set limitations and anharmonicity effects. A potential energy distribution (PED) of the normal modes for each isomer of 2′-hydroxyacetophenone azine was computed in terms of internal coordinates with the Gar2ped program [26].

3. Results and discussion

3.1. Calculated properties of EE-trans and EE-gauche conformers

The calculations resulted in eleven stationary points on the potential energy surface of APA at the DFT/B3LYP/6-311++G(2d,2p) level of theory (only the configurations in which the methyl group is in a *trans* position to the $(C—C(O))_{ring}$ bond were taken into account). The two most stable structures (I, II) correspond to *E*/*E* configuration, they are presented in Fig. 1. The next conformer (taking as a criterion the stability) has Z/Z configuration and is by ca. 31 kJ mol^{-1} less stable than conformers I and II; the structures of all optimized conformers are presented in Fig. 1, Supporting material. The calculations also demonstrated the stability of a keto tautomer of conformer I in which one hydrogen atom in intramolecular O—H···N hydrogen bond is transferred from an oxygen atom to a nitrogen atom (Fig. 2). The keto tautomer of I is by 19.94 kJ mol^{-1} less stable than the enol form. The calculations did not result in minimum corresponding to a keto structure in which two protons are transferred to the N atoms. This is in accord with earlier reported experimental and theoretical data for symmetric Schiff bases that demonstrated single proton transfer process during excitation of symmetric Schiff bases [27,28].

In Table 1, the calculated geometrical parameters for I and II are presented and compared with the experimental values reported for crystalline APA [18,20]. The calculated value of τ_1 angle (φ $C_{10}N_{11}N_{28}C_{26}$) equals to −180.0° for I and to −155.4° for II which is characteristic for *trans* and *gauche* conformers, respectively. In Table 2, the energies of the two conformers are compared; the energy minimum corresponding to a I-*trans* conformer lies 0.66 kJ mol^{-1} above that corresponding to a II-*gauche* one when ZPVE is not taken into account but after including ZPVE correction the minimum corresponding to a I-*trans* conformer is 0.09 kJ mol^{-1} below that corresponding to a II-*gauche* one. ZPVE correction leads to the reverse of the stability order of the two conformers.

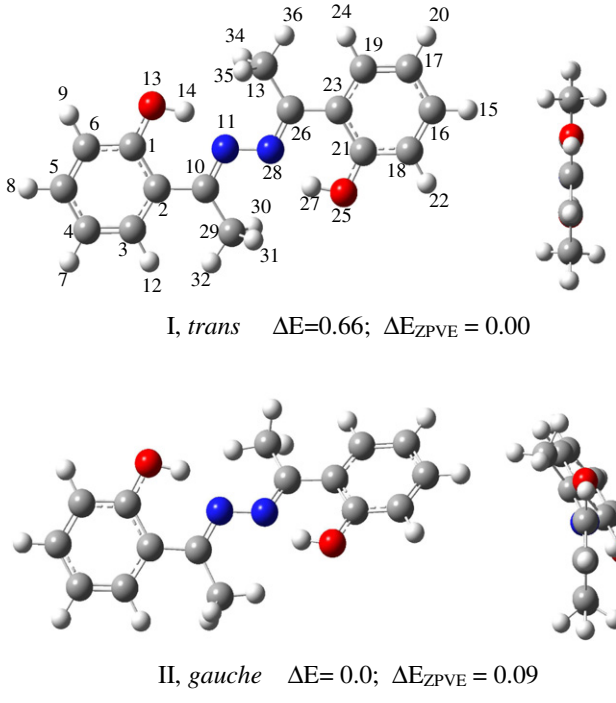

Fig. 1. DFT/B3LYP/6-311++G(2d,2p) optimized *s-trans* and *gauche* conformers of *E*/*E* configuration of 2′-hydroxyacetophenone azine.

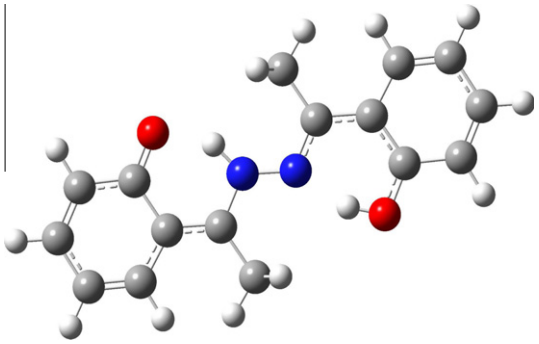

Fig. 2. The DFT/B3LYP/6-311++G(2d,2p) optimized structure of a keto tautomer of a *s-trans* conformer 2′-hydroxyacetophenone azine.

As one can see in Table 1, the experimental values reported for crystalline APA [20] show good agreement with the calculated parameters for I indicating that the molecule in solid state shows *s-trans* conformation. The largest discrepancies concern the OH and H···N distances which is due to uncertainty of H position determination by X-ray study. The comparison of the geometrical parameters for I and II demonstrates that the rotation of the [(o-OHAr)CMe=N—]$_2$ grouping around N—N bond by ca. 25° (τ_1 angle changes from −180° to −155.4°) when going from a *trans* to a *gauche* conformation is accompanied by rotation of two CH_3 groups around C—C bond by ca. 180°. The dihedral φ ($C_2C_{10}C_{29}H_{32}$) and φ ($C_{23}C_{26}C_{33}H_{36}$) angles change from 0.96°, −0.94° to −176.9° (for both angles) when going from a *trans* to a *gauche* form. This is accompanied by the change of the dihedral φ ($N_{11}N_{28}C_{26}C_{33}$), φ ($N_{28}N_{11}C_{10}C_{29}$) angles from ca. 0° to 6.3°. There are also other small structural differences in geometrical parameters of the H_3C—C=N—N=C—CH_3 grouping between *trans* and *gauche* conformers as can be seen in Table 1.

Table 2
Relative energies, kJ mol^{-1}, (not corrected, ΔE, and corrected for zero-point vibrational contributions, ΔE_{ZPVE}), and estimated populations for a *trans* and a *gauche* conformers of 2′-hydroxyacetophenone azine.

Conformer	2′-hydroxyacetophenone azine		Population (%)[a]	
	ΔE	ΔE_{ZPVE}	E	E_{ZPVE}
I Trans	0.66	0 (−879.261192)[b]	28	34
II Gauche	0 (−879.550782)[b]	0.09	72	65

[a] According to Boltzmann distribution at 60 °C (temperature of deposition).
[b] In parantheses the values of electronic energy, E, or electronic energy with zero-point contribution, E_{ZPVE}, in hartree are given.

Fig. 3 presents the potential-energy profile for internal rotation around the N—N bond (C=N—N=C dihedral angle) in APA calculated at the DFT/B3LYP/6-311++G(2d,2p) level of approximation; the profile is based on energy values of the potential minima (not corrected for ZPVE). As one can see the minima corresponding to *gauche* configuration are separated from the minimum corresponding to a *s-trans* conformer by very low barrier, 1.06 kJ mol^{-1}; the energy difference between the two minima corresponding to *trans* and *gauche* forms is also very low (0.66 kJ mol^{-1}). The zero-point corrected electronic energies will slightly modify the energy profile, however the general picture, i.e. small energy difference and very low energy barriers between the two conformers, will remain.

In Table 2, the electronic energies, zero-point corrected electronic energies and relative abundances for the optimized I and II conformers are collected. The relative abundances of the two conformers were estimated from Boltzmann distribution at the deposition temperature 333 K, on the basis of their calculated relative energies (both ΔE and ΔE(ZPVE) were taken into account) and taking into account the weighting factors (degeneracy) for the *trans* and *gauche* structures as equal to 1 and 2. The obtained results indicate that both *trans* and *gauche* conformers should be present

Table 1
The comparison of the DFT/B3LYP/6-311++G(2d,2p) calculated geometrical parameters for a *trans* and *gauche* conformers of 2′-hydroxyacetophenone azine with the reported crystallographic data.

	Trans	Gauche	Ref. [18]	Ref. [20]
r $N_{11}N_{28}$	1.374	1.378	1.401(5)	1.394(4)
r $N_{11(28)}C_{10(26)}$	1.305	1.300	1.302(6), 1.285(6)	1.300(5), 1.295(5)
r $C_{10(26)}C_{2(23)}$	1.467	1.469	1.478(6), 1.477(7)	1.464(5), 1.460(6)
r $C_{10(26)}C_{29(33)}$	1.507	1.506	1.477(7), 1.493(8)	1.497(5), 1.495(5)
r $C_{1(21)}O_{13(25)}$	1.340	1.343	1.347(7), 1.355(6)	1.346(5), 1.352(5)
r $O_{13(25)}H_{14(27)}$	0.999	0.993		0.8200
r $O_{13(25)}H_{14(27)}\cdots N_{11(28)}$	1.640	1.678	1.579, 1.862	1.80
θ $N_{11(28)}N_{28(11)}C_{26(10)}$	116.49	118.12	115.1(4), 115.4(4)	115.8(3), 115.7(3)
θ $N_{11(28)}C_{10(26)}C_{2(23)}$	117.14	117.40	115.8(4), 116.3 (5)	116.5(4)
θ $N_{11(28)}C_{10(26)}C_{29(33)}$	120.90	123.37	124.8(5), 123.6(5)	124.0(4), 123.2(4)
θ $C_{2(23)}C_{10(26)}C_{29(33)}$	121.95	119.23	122.6(5), 122.8(5)	119.6(4), 120.3(4)
θ $C_{2(23)}C_{1(21)}O_{13(25)}$	122.47	122.43	122.6(5), 122.8(5)	122.1(4), 122.0(4)
θ $C_{1(21)}C_{2(23)}C_{10(26)}$	121.36	122.02	121.9(5), 121.8(5)	122.1(4), 122.3(4)
θ $C_{21(1)}O_{25(13)}H_{27(14)}$	106.04	106.28		109.5
θ $O_{13(25)}H_{14(27)}\cdots N_{11(28)}$	148.78	148.08	141.5, 155.8	146, 147
φ $C_{10}N_{11}N_{28}C_{26}$	−180.00	−155.41	177.0	−177.9(4)
φ $N_{11}N_{28}C_{26}C_{33}$	−0.063	6.33		−0.6(6)
φ $N_{28}N_{11}C_{10}C_{29}$	−0.072	6.34		−0.2(5)
φ $N_{11}N_{28}C_{26}C_{23}$	179.93	−174.15		179.9(3)
φ $N_{28}N_{11}C_{10}C_2$	−179.92	−174.14		−179.2(3)
φ $N_{11}C_{10}C_2C_1$	−0.35	3.39		2.7(5)
φ $N_{28}C_{26}C_{23}C_{19}$	0.38	3.40		2.2(5)
φ $C_{29}C_{10}C_2C_1$	−179.63	−177.064		−176.4(4)
φ $C_{33}C_{26}C_{23}C_{21}$	−177.055	−179.63		−177.4(4)
φ $C_2C_{10}C_{29}H_{32}$	0.96	−176.93		
φ $C_{23}C_{26}C_{33}H_{36}$	−0.94	−176.96		
φ $C_2C_1O_{13}H_{14}$	−0.22	0.15		
φ $C_{23}C_{21}O_{25}H_{27}$	−0.23	−0.18		

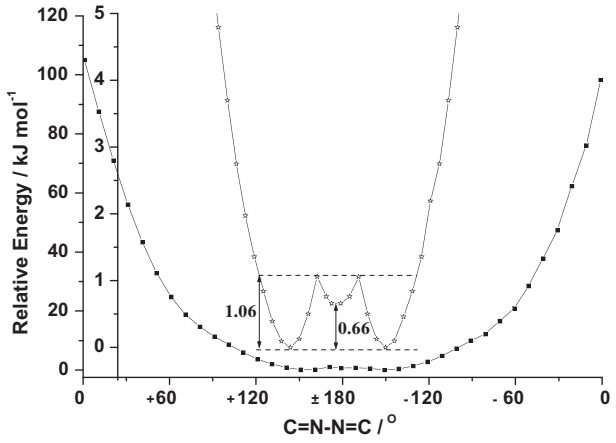

Fig. 3. DFT/B3LYP/6-311++G(2d,2p) calculated potential-energy profile for internal rotation around the N—N bond.

in an argon matrix after deposition of the vapour above solid APA and, moreover, they are expected to exhibit reversible interconversion at matrix temperature due to the very low barrier between them [22].

4. Infrared spectra

APA in a *trans* form has C_{2h} symmetry, and its vibrations can thus be distributed as $\Gamma_{vib} = 35A_g + 34B_u + 17A_u + 16B_g$. When the [(o-OHAr)CMe=N—] grouping is rotated around a C=N—N=C angle to a *gauche* conformation all the symmetry elements are lost and all APA vibrations become active in infrared spectrum. However the intensities of all normal modes that became active in a *gauche* conformer are very weak (see Table 1, Supporting material), so, the spectra of the two forms are, in fact, quite similar.

In Table 3 the experimental frequencies are compared with the calculated ones for the *s-trans* and *gauche* conformers; in Fig. 4 the experimental and theoretical spectra are presented. The simulated, theoretical IR spectrum was built by adding the calculated individual spectra of the two conformers scaled by the corresponding estimated populations at 333 K. One has to remember that due to the very low barrier between the two conformers and small difference between their electronic energies one can expect conformational equilibration in the matrix at 20 K [22]. Low energy barriers promote also the relaxation of the higher energy local minima into more stable structures, this effect is known as the conformational cooling effect [29,30]. The two conformers are characterized by very similar set of frequencies and the simulated spectrum reproduces relatively well the observed one in the 1800–400 cm^{-1} region. In Fig. 4 are presented the 1675–1400 cm^{-1} and 1425–1150 cm^{-1} spectral regions of the APA/Ar matrix at 9 K (a), after its annealing to 32 K (b) and then after cooling down again to 9 K (c). One can see clearly the reversible temperature dependence of a number of bands pairs which indicates a reversible interconversion of the two conformers at matrix temperatures. The comparison of the experimental spectra with the calculated ones for the *s-trans* and *gauche* conformers allowed us to assign unambigously all the component bands whose intensities increase at higher matrix temperature to *s-trans* conformer and those whose intensities decrease to a *gauche* one. For example, the 1511, 1516 cm^{-1}

Table 3
Comparison of the experimental and calculated frequencies (cm^{-1}) and intensities (km mol^{-1}) for a *trans* and *gauche* conformers of 2′-hydroxyacetophenone azine; the results of potential energy distribution are also given.

[16]	Trans				Gauche			
	Ar matrix	Calculated			Ar matrix	Calculated		
ν_{obs}	ν_{obs}	$\nu_{harm.}$	I	PED %	ν_{obs}	$\nu_{harm.}$	I	PED[a] %
		3165	29	83νCH		3153	19	95νCH
		3143	28	95νCH		3143	28	89νCH
		3136	11	89νCH		3135	14	100νCH
					2816–2651	3122	17	66νOH + 24νCH
		3120	21	71νCH$_3$ + 14νCH		3119	14	86νCH
	2651–2555	3004	316	71νCH$_3$ + 24νOH	2816–2651	3104	1338	97νOH
		2995	1005	76νOH + 22νCH$_3$		2999	19	91νCH$_3$
	1624.1 w	1627	259	36νCC$_{ring}$+18δCOH	1627.6 w	1627	235	38νCC$_{ring}$ + 14δCOH
1605 vs	1611.7 s	1605	202	10νCN + 16νCC$_{ring}$ + 12δCOH + 7δCCC(N)	1608.2 s	1605	280	20νCN + 12νCC$_{ring}$ + 8δCOH + 8δCCC(N)
1569 vs	1563.3 m	1560	367	46νCN + 9δCOH	1563.3 m	1574	286	38νCN + 10δCOH
1497 s	1501.7 w	1516	62	22νCC$_{ring}$ + 22δCOH + 16δCH$_{ring}$	1492.4 w	1511	45	22δCOH + 19νCC$_{ring}$ + 18δCH$_{ring}$
		1485	56	50δCH$_3$				
	1454.7 w	1459	17	90δCH$_3$	1450.1 w	1460	56	30δCH$_3$ + 15δCH$_{ring}$
1439 s	1444.9 vw	1446	101	33δCH$_{ring}$ + 12νCN	1447.5 w	1446	92	38δCH$_3$ + 12νCN
	1396.8 w	1424	128	20δCOH + 18δCH$_3$ + 14δCH$_{ring}$	1400.4 vw	1432	40	28δCOH + 28δCH$_{ring}$
1362 s	1368.6 m	1388	28	90δCH$_3$	1368.6 m	1383	38	82δCH$_3$
1300 s	1305.6 vs	1308	111	24νCO + 18νCC(N)+14δCC$_{ring}$	1305.6 vs	1307	136	26νCO + 14νCC(N)+14δCC$_{ring}$
1247 s	1249.9 w	1252	171	30νCC$_{ring}$ + 20νCO + 10δCH$_{ring}$	1253.8 m	1254	103	30νCC$_{ring}$ + 24νCO + 16δCH$_{ring}$
	1239.3 w	1242	69	28δCH$_{ring}$ + 22νCC$_{ring}$	1231.8 w	1240	106	36νCC$_{ring}$ + 18δCH$_{ring}$ + 17δCOH
1158 m	1165.2 w	1169	62	50δCH$_{ring}$ + 14νCC$_{ring}$	1161.4 w	1166	56	52δCH$_{ring}$ + 12νCC$_{ring}$
1135 w	1129.8 vw	1131	13	38δCH$_{ring}$ + 12νCC$_{ring}$	1129.8 vw	1130	15	38δCH$_{ring}$ + 12νCC$_{ring}$
1031 w					1038.5 vw	1040	11	46δCH$_3$ + 17γCC(C)N
839 s	840.8 w	896	76	97γCOH	830.2 vw	869	47	66γCOH + 14γCH$_{ring}$
	820.2 vw	858	16	31γCCH$_{ring}$ + 17τCCCC$_{ring}$ + 15γCCO	820.2 vw	859	45	33γCH$_{ring}$ + 14γCCO + 14τCCCC$_{ring}$ + 12γCOH
	805.1 vw	840	16	40δCC$_{ring}$ + 16νCO	807.3 vw	840	17	40δCCC$_{ring}$ + 16νCO
758 s		750	32	46τCCCC$_{ring}$ + 18γCCN + 16γCCO	753.2 s	751	31	36τCCCC$_{ring}$ + 24γCCO + 18γCCC(N)+16γCH$_{ring}$
	749.7 m	746	103	54γCCH$_{ring}$ + 20γCCO	751.9 vs	749	95	26γCCC(N)+24τCCCC$_{ring}$ + 18γCCH
662 w	662.4 w	663	45	44δCCN + 21δCC$_{ring}$	664.0 w	669	46	34δCCN + 23δCCC$_{ring}$ + 14τCCNN

[a] Only PED values greater than 7% are presented. In the Gar2ped program that was used to calculate PED the internal coordinates were determined as follows: all stretches, methyl group deformations, C_6 ring deformations, C_rC_r (H)C_r, C_rC_r(O)C_r and C_rC_r(C)C_r deformations, C_r–C(C)=N deformations, COH in plane deformation and torsions around C—C(H_3), C_r—C, C=N and N—N bonds (r indicates ring C atom). Definition of coordinates: ν, bond stretching, δ, bending, γ, out of (ring) plane bending, τ, torsion. All the contributions to PED present antisymmetric vibrations of two corresponding coordinates in the two halves of azine. Experimental intensities are presented in qualitative terms: vs, very strong; s, strong; m, medium; w, weak; vw, very weak.

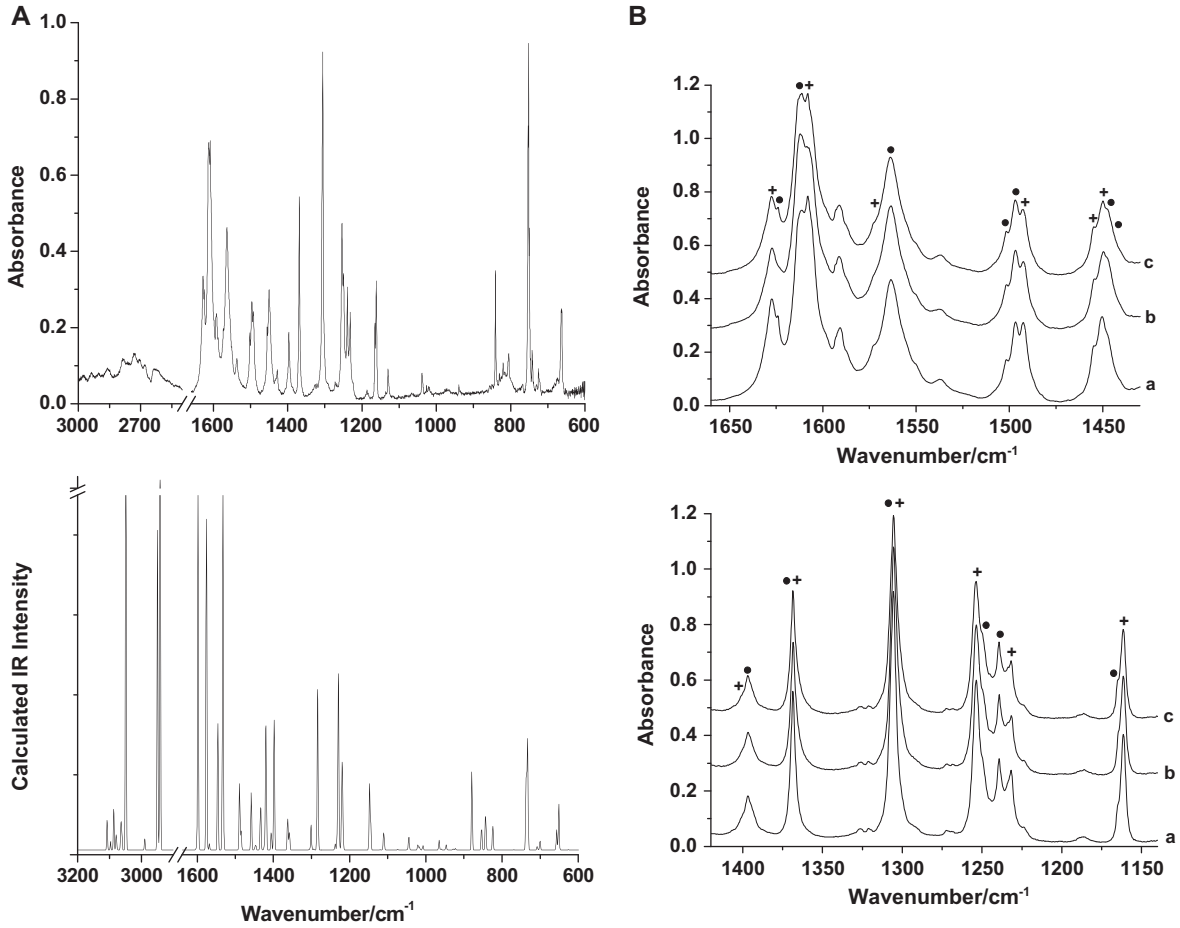

Fig. 4. (A) Infrared spectra of 2′-hydroxyacetophenone azine trapped in an argon matrix (upper curve) and simulated spectrum obtained by summing the calculated spectra for a *trans* and a *gauche* conformers at the DFT/B3LYP/6-311++G(2d,2p) level of theory, scaled by their estimated Boltzmann populations at 333 K. (B) The 1670–1425, 1400–1150 cm^{-1} regions in the spectra of APA/Ar matrix. Spectra were recorded directly after matrix deposition at temperature 9 K (a), after heating up the matrix to 32 K (b) and after cooling the matrix to 9 K (c). The bands due to a *gauche* and *s-trans* conformers are marked by "+" and "•", respectively.

calculated frequencies of the *gauche* and *s-trans* conformers, are assigned in the experimental spectrum to the bands at 1492.4 and 1501.7 cm^{-1}, respectively. The intensity of the 1492.4 cm^{-1} component due to *a gauche* form decreases and that at 1501.7 cm^{-1} due to a *trans* one increases after matrix annealing. The observed spectral characteristics indicates that a *trans* conformer is less stable than a *gauche* one as indicated by the DFT/B3LYP/6-311++G(2d,2p) calculated electronic energy difference between the two conformers however without zero-point correction. Taking into account ZPVE correction leads to the reverse of the energy order, so, the calculations do not reproduce correctly the small energy difference between the two conformers.

4.1. The COH group vibrations

The COH groups serve as proton donors to N atoms forming two internal O—H···N hydrogen bonds. The calculations show that the frequencies of the COH groups vibrations are very sensitive to the rotation around C=N—N=C angle. The two νOH vibrations are calculated to appear at ca 3000 cm^{-1} for a *trans* isomer and at ca. 3100 cm^{-1} for a *gauche* one; in *trans* conformer the vibration is strongly coupled with νCH_3 whereas in a *gauche* one a weak coupling between one of the two νOH vibrations and νCH vibration occurs. The analysis of the experimental spectra allowed us to assign a broad, diffuse band with some structure in the 2650–2555 cm^{-1} region to the OH stretching vibration of *s-trans* conformer and a similar band extending in the 2815–2650 cm^{-1} region to the OH stretching of a *gauche* one. The shape and the position of these bands are similar to the characteristics of the corresponding bands observed for the ortho-hydroxy acylaromatic Schiff bases containing chelate ring with intramolecular O—H···N bond [31]. One may note that the two bands appear in the lower frequency region than that predicted by calculations. It is a known fact that the matrix material, even as inert as solid argon, strongly effects the structure and, in consequence, the vibrations of strongly hydrogen bonded systems. The most spectacular example is the ammonia-hydrogen chloride complex for which the hydrogen stretching vibration was identified at 2084 cm^{-1} in solid Ne and at 1370.9 cm^{-1} in solid argon [32–34].

The δ(COH) vibrations in both conformers are strongly coupled with the νCN, νCC_{ring}, and δCH_{ring} vibrations; the normal modes involving the C=N, CC_{ring} stretching and COH, CH_{ring} bending vibrations occur in the 1630–1400 cm^{-1} region (Table 3); however the effect of conformational change on these vibrations is less clear than on νOH and δ(OH) ones.

The γOH mode is calculated to occur at 896 cm^{-1} in a *trans* and at 869 cm^{-1} in a *gauche* conformer (in a *gauche* conformer γCH_{ring} vibration gives a small contribution to γCOH), and the corresponding bands are identified at 840.8 cm^{-1} and at 830.2 cm^{-1}, respectively. The higher γCOH frequency for a *trans* than for a *gauche* conformer is corresponding with the lower νOH value of the first conformer. The relative values of the νOH frequencies as well as γOH ones of the two conformers indicate that the intramolecular O—H···N bond is stronger in a *trans* form than in a *gauche* one.

The weakening of the O—H···N hydrogen bond in a *trans* form is also responsible for the lower frequency of the vibration with relatively large contribution of the C—O stretching vibration in this conformer as compared to a *gauche* one (1249.9, 805.1 cm^{-1}, for a *trans* versus 1253.8, 807.3 cm^{-1} for a *gauche*). The stronger intramolecular O—H···N bond might be due to a stronger conjugation of the two halves of the azine in a *trans* form.

The effect of rearrangement on the other frequencies of APA is less obvious.

5. Conclusions

The DFT/B3LYP/6-311++G(2d,2p) calculations show that the two lowest energy minima on the potential energy surface of 2′-hydroxyacetophenone azine (APA) correspond to two C=N—N=C conformational isomers of *E*/*E* configuration of APA, namely to s-*trans* conformer and to a *gauche* one. The performed calculations demonstrate that the two conformers have very close energies and are separated by very low barrier. A *gauche* conformer is more stable by 0.66 kJ mol^{-1} taking electronic energies (E) as a criterion of stability, however including ZPVE correction (E_{ZPVE}) leads to a reverse of the energy order and *s-trans* becomes more stable by 0.09 kJ mol^{-1} than a *gauche* conformer. Potential-energy profile around C=N—N=C angle, based on E, results in energy barrier of 1.06 kJ mol^{-1} when going from a *gauche* conformer to a *s-trans* one.

FTIR spectra of APA isolated in argon matrices evidence that both s-*trans* and *gauche* conformers are present in the matrix and exhibit reversible interconversion at matrix temperatures 9–32 K. The comparison of the experimental spectra with the theoretical ones calculated for the two conformers and reversible temperature dependence of the bands intensities allowed us to obtain the spectroscopic characteristics of a *s-trans* and a *gauche* conformer. The temperature dependence of the bands intensities also demonstrated that a *gauche* isomer is more stable than a *trans* one. The spectra analysis shows that most sensitive to conformational rearrangement are hydrogen bond vibrations. The intramolecular O—H···N hydrogen bond is weakened when APA is converted from a *trans* to a *gauche* conformer.

Acknowledgements

The research was supported by the Polish Ministry of Science and Higher education (Grant N N204 020 340837). We gratefully acknowledge a grant of computer time from the Wrocław Center for Networking and Supercomputing (WCSS).

Appendix A. Supplementary material

Supplementary data associated with this article can be found, in the online version, at doi:10.1016/j.molstruc.2010.04.017.

References

[1] V.M. Kolb, A.C. Kuffel, H.O. Spiwek, T.E. Janota, J. Org. Chem. 54 (1989) 2771.
[2] T.W. Bell, A.T. Papoulis, Angew. Chem. Int. Ed. Engl. 31 (1992) 749.
[3] P. Espinet, J. Etxebarria, M. Marcos, J. Perez, A. Remon, J.L. Serrano, Angew. Chem. Int. Ed. Engl. 28 (1989) 1065.
[4] D.S. Dudis, A.T. Yeates, D. Kost, D.A. Smith, J. Medrano, J. Am. Chem. Soc. 115 (1993) 8770.
[5] J. Barluenga, M.J. Iglesias, V. Gotor, J. Chem. Soc. Chem. Commun. (1987) 582. and references therein.
[6] I. Ikeda, Y. Kogame, M. Okahara, J. Org. Chem. 50 (1985) 3640.
[7] D. Bardley, Science 261 (1993) 1272.
[8] G.S. Chen, J.K. Wilbur, Ch.L. Barnes, R. Glaser, J. Chem. Soc. Perkin Trans. 2 (1995) 2311.
[9] W. Tang, Y. Xiang, A. Tong, J. Org. Chem. 74 (2009) 2163.
[10] G.S. Chen, M. Anthamatten, Ch.L. Barnes, R. Glaser, J. Org. Chem. 59 (1994) 4336.
[11] G.S. Chen, M. Anthamatten, Ch.L. Barnes, R. Glaser, Angew. Chem. Int. Ed. Engl. 33 (1994) 1081. and references therein.
[12] T.G.D. van Schalkwyk, A.M. Stephen, ARKIVOC 13 (2005) 109.
[13] V.B. Kobychev, N.M. Vitkovskaya, N.V. Pavlova, E.Yu. Schmidt, B.A. Trofimov, J. Struct. Chem. 45 (2004) 748.
[14] F. Blanco, I. Alkorta, J. Elguero J. Mol. Struct. (THEOCHEM) 847 (2007) 25.
[15] I. Alkorta, F. Blanco, J. Elguero ARKIVOC 7 (2008) 48.
[16] B.A. El-Sayed, M.M. Abo Aly, A.A.A. Emara, S.M.E. Khalil, Vibrational Spectr. 30 (2002) 93.
[17] A.H. Ammar, B.A. El-Sayed, E.A. El-Sayed, J. Mater. Sci. 37 (2002) 3255.
[18] H. Höpfl, N. Farfán, Can. J. Chem. 76 (1998) 1853.
[19] M. Ziółek, K. Filipczak, A. Maciejewski, Chem. Phys. Lett. 464 (2008) 181. and references therein.
[20] X.S. Tai, J. Xu, Y.M. Feng, Z.P. Liang, Acta Cryst. E64 (2008) 0905.
[21] M.M. Abo Aly, Spectrochim. Acta A 55 (1999) 1711.
[22] A.J. Barnes, J. Mol. Struct. 113 (1984) 161.
[23] B.S. Furnuss, A.J. Hannaford, P.W.G. Smith, A. Tatchell, Vogel's Textbook of Practical Organic Chemistry, Longmans, New York, 1989.
[24] M.J. Frisch, G.W. Trucks, H.B. Schlegel, G.E. Scuseria, M.A. Robb, J.R. Cheeseman, J.A. Montgomery, Jr., T. Vreven, K.N. Kudin, J.C. Burant, J.M. Millam, S.S. Iyengar, J. Tomasi, V. Barone, B. Mennucci, M. Cossi, G. Scalmani, N. Rega, G.A. Petersson, H. Nakatsuji, M. Hada, M. Ehara, K. Toyota, R. Fukuda, J. Hasegawa, M. Ishida, T. Nakajima, Y. Honda, O. Kitao, H. Nakai, M. Klene, X. Li, J.E. Knox, H.P. Hratchian, J.B. Cross, V. Bakken, C. Adamo, J. Jaramillo, R. Gomperts, R.E. Stratmann, O. Yazyev, A.J. Austin, R. Cammi, C. Pomelli, J.W. Ochterski, P.Y. Ayala, K. Morokuma, G.A. Voth, P. Salvador, J.J. Dannenberg, V.G. Zakrzewski, S. Dapprich, A.D. Daniels, M.C. Strain, O. Farkas, D.K. Malick, A.D. Rabuck, K. Raghavachari, J.B. Foresman, J.V. Ortiz, Q. Cui, A.G. Baboul, S. Clifford, J. Cioslowski, B.B. Stefanov, G. Liu, A. Liashenko, P. Piskorz, I. Komaromi, R.L. Martin, D.J. Fox, T. Keith, M.A. Al-Laham, C.Y. Peng, A. Nanayakkara, M. Challacombe, P.M.W. Gill, B. Johnson, W. Chen, M.W. Wong, C. Gonzalez, J.A. Pople, Gaussian 03, Revision C.02, Gaussian, Inc., Wallingford CT, 2004.
[25] S.F. Boys, F. Bernardi, Mol. Phys. 19 (1970) 553.
[26] J.M.L. Martin, C. Van Alsenoy, Gar2ped, University of Antwerp, 1995.
[27] K. Kownacki, Ł. Kaczmarek, A. Grabowska, Chem. Phys. Lett. 210 (1993) 373.
[28] K. Kownacki, A. Mordziński, R. Wilbrandt, A. Grabowska, Chem. Phys. Lett. 227 (1994) 270.
[29] I.D. Reva, A.J. Lopes Jesus, M.T. Rosado, R. Fausto, M.E. Eusébio, J.S. Redinha, Phys. Chem. Chem. Phys. 8 (2006) 5339.
[30] A. Borba, A. Gómez-Zavaglia, R. Fausto, J. Mol. Struct. 794 (2006) 196.
[31] J. Pająk, G. Maes, W.M. De Borggraeve, N. Boens, A. Filarowski, J. Mol. Struct. 844–845 (2007) 83.
[32] A.J. Barnes, T.J. Beech, Z. Mielke, J. Chem. Soc. Faraday Trans. 2 (80) (1984) 465.
[33] A.J. Barnes, A.C. Legon, J. Mol. Struct. 448 (1998) 101.
[34] L. Andrews, X. Wang, Z. Mielke, J. Phys. Chem. A 105 (2001) 6054.